

## Investigation of cluster structure of ${}^9\text{Be}$ from high precision elastic scattering data

S. K. Pandit,<sup>1,\*</sup> V. Jha,<sup>1,†</sup> K. Mahata,<sup>1</sup> S. Santra,<sup>1</sup> C. S. Palshetkar,<sup>1</sup> K. Ramachandran,<sup>1</sup> V. V. Parkar,<sup>2,‡</sup> A. Shrivastava,<sup>1</sup> H. Kumawat,<sup>1</sup> B. J. Roy,<sup>1</sup> A. Chatterjee,<sup>1</sup> and S. Kailas<sup>1</sup>

<sup>1</sup>*Nuclear Physics Division, Bhabha Atomic Research Centre, Mumbai-400085, India*

<sup>2</sup>*Department of Nuclear and Atomic Physics, Tata Institute of Fundamental Research, Mumbai-400005, India*

(Received 30 May 2011; revised manuscript received 15 July 2011; published 6 September 2011)

The cluster structure of  ${}^9\text{Be}$  has been investigated through high precision elastic scattering cross-section measurements of a  ${}^9\text{Be} + {}^{208}\text{Pb}$  system at below barrier energies,  $E = 24\text{--}34$  MeV. The observed deviation from the Rutherford scattering can only be explained by an  $n + {}^8\text{Be}$  cluster description of  ${}^9\text{Be}$ , whereas the  $\alpha + {}^5\text{He}$  cluster picture fails to explain the measured data, indicating the dominance of the  $n + {}^8\text{Be}$  cluster structure of  ${}^9\text{Be}$ . In addition to sequential and direct breakup, the coupling effect of one neutron stripping on elastic scattering is significant even at 10 MeV below the barrier. The sensitivity of the high precision elastic scattering data to the cluster structure of  ${}^9\text{Be}$  has been demonstrated.

DOI: [10.1103/PhysRevC.84.031601](https://doi.org/10.1103/PhysRevC.84.031601)

PACS number(s): 21.60.Gx, 24.10.Eq, 25.70.Bc, 25.70.De

Clustering is a general phenomena that is observed over a wide range of physical scales and in diverse fields such as the aggregation of galaxies in the universe or the existence of gene clusters in complex biological systems. In the nuclear domain, clustering observed in light nuclei elucidates on their structure that leads to a greater understanding of the underlying correlations of nucleons. It is well known that the light weakly bound nuclei  ${}^6,7\text{Li}$  have predominantly  $\alpha + d$  and  $\alpha + t$  cluster structures, respectively, but the cluster structure of  ${}^9\text{Be}$  is still not clear. Study of the  ${}^9\text{Be}$  cluster structure is of recent interest, especially for the astrophysically important  ${}^{12}\text{C}$  formation via the  $\alpha + \alpha + n \rightarrow {}^9\text{Be}$  channel followed by the  ${}^9\text{Be}(\alpha, n){}^{12}\text{C}$  reaction [1]. At high energies, the experimental observation of the anomalous modification of the nucleon structure function  $F_2$  in the  ${}^9\text{Be}$  nucleus has been ascribed to the clustering effects of the  ${}^9\text{Be}$  nucleus [2,3]. Further, the description of the  ${}^9\text{Be}$  nucleus in terms of a neutron with two  $\alpha$ -particle cores provides pathways to greater understanding of halo and molecular structures in three-body systems [4]. At low energies, the cluster structure is usually studied by the measurement of different breakup channels and is correlated with the possible cluster configurations. In the case of  ${}^9\text{Be}$ , apart from the direct three-body  $\alpha$ - $\alpha$ - $n$  decay, the breakup may occur through either  ${}^9\text{Be} \rightarrow n + {}^8\text{Be}$  or  ${}^9\text{Be} \rightarrow \alpha + {}^5\text{He}$  routes. However, the lifetimes of  ${}^8\text{Be}$  and  ${}^5\text{He}$  nuclei are  $10^{-16}$  s and  $10^{-21}$  s, respectively, which is too small to detect them directly. As a result, in a breakup measurement, only two  $\alpha$ 's and an  $n$  can be detected, and it is experimentally difficult to distinguish among the intermediate paths within the interaction regions.

The experimentally observed  ${}^9\text{Be}$  low-energy spectrum above the  $\alpha$ - $\alpha$ - $n$  threshold of 1.57 MeV consists of  $\frac{1}{2}^{\pm}$ ,  $\frac{3}{2}^{\pm}$ , and  $\frac{5}{2}^{\pm}$  resonances. These resonance states could contribute to processes bridging the  $A = 5, 8$  instability gaps in

heavy element nuclear synthesis under suitable astrophysical environments. Although the theoretical calculations are able to reproduce the measured excited energy levels reasonably well, their decay properties have not been established. There have been several recent measurements of  ${}^9\text{Be}$  cluster breakup [5–8], and attempts have been made to quantify the contribution of decay components for the low-lying excitation spectrum of  ${}^9\text{Be}$ . In addition, the cluster structure of  ${}^9\text{Be}$  has been studied by measuring its excited states by the  ${}^9\text{Be}(\gamma, n)$  [9] or  ${}^9\text{Be}(e, e')$  [10] techniques, and then reproducing those excited states by different cluster model calculations. Even though the  ${}^9\text{Be}$  nucleus is more accurately described by a three-body  $\alpha + \alpha + n$  cluster structure, the simple two-body  $\alpha + {}^5\text{He}$  [ $\alpha + (\alpha + n)$ ] or  $n + {}^8\text{Be}$  [ $n + (\alpha + \alpha)$ ] cluster configuration can be effectively used in calculations to explain reaction mechanisms. While the positive-parity states can be reproduced by the  $n + {}^8\text{Be}$  [11] cluster model rather well, there is still uncertainty about the nature of negative-parity states and the importance of  $\alpha + {}^5\text{He}$  [12–14] cluster structures in their decay. In a recent calculation, a dynamic evolution from  $\alpha + {}^5\text{He}$  at small distances to an  $n + {}^8\text{Be}$  cluster structure at large distances has been shown for the two low-lying resonances  $\frac{1}{2}^+$  [15] and  $\frac{5}{2}^-$  [16].

The low-lying resonances and nonresonant continuum arising due to small breakup threshold of a weakly bound nucleus have significant coupling effects on the elastic scattering. More specifically, a strong excitation of the low-lying  $E1$  strength is possible even at below barrier energies, which can be a sensitive probe of the large distance radial wave function. The strong coupling between the ground state and the dipole states in the continuum leads to a deviation of the elastic cross section at backward angles from the Rutherford value even at below barrier energies. At energies around the Coulomb barrier, the influence of the breakup process on elastic scattering and fusion channels has been discussed extensively in the literature [17–19]. A cluster model analysis considering  ${}^9\text{Be}$  as an  $\alpha + {}^5\text{He}$  cluster model [18] to explain the elastic scattering angular distribution of the  ${}^9\text{Be} + {}^{208}\text{Pb}$  system around and above the Coulomb barrier gives good agreement with the measured elastic scattering angular distribution [20]. However,

\* sanphysics@gmail.com

† vjha@barc.gov.in

‡ Present address: Departamento de Física Aplicada, Universidad de Huelva, E-21071, Spain.

the model calculation gives only one-third of the measured breakup cross section for the above system [21]. An alternative model calculation considering  ${}^9\text{Be}$  as an  $n + {}^8\text{Be}$  cluster [22] gives reasonably good agreement with the measured fusion cross section for the  ${}^9\text{Be} + {}^{209}\text{Bi}$  system.

While it is difficult to conclude on the cluster structure of  ${}^9\text{Be}$  from simple elastic scattering or fusion measurements around the barrier, precision elastic scattering measurement at low energies is expected to bring out the signature of different cluster structures due to the dominance of coupling effects of low-lying dipole states. With this motivation, we have measured high precision elastic scattering data for a  ${}^9\text{Be} + {}^{208}\text{Pb}$  system at energies below the Coulomb barrier at the backward angle. The effects of dipole coupling to the low-lying breakup states and one-neutron transfer reactions on elastic scattering cross sections are presented. In addition to the analysis of the present precision elastic data, calculations have been performed to explain the measured breakup and one-neutron transfer cross sections of Woolliscroft *et al.* [21].

The experiment was carried out using the  ${}^9\text{Be}$  beam from the 14UD BARC-TIFR Pelletron facility. The enriched  ${}^{208}\text{Pb}$  (>98%) target of  $\sim 200 \mu\text{g}/\text{cm}^2$  thickness with a backing of  ${}^{12}\text{C}$  of  $\sim 35 \mu\text{g}/\text{cm}^2$  thickness was used. Projectile-like particles were detected by the  $\Delta E$ - $E$  telescopes consisting of Si surface-barrier detectors. Major attention was given in this experiment to keep the measurement uncertainties <0.5%. To achieve this, the following detector arrangement was made: Two pairs of identical telescopes were placed symmetrically to the left and right of the incident beam at  $\pm 40^\circ$  and  $\pm 160^\circ$ .  $\Delta E$  detectors of thicknesses  $\sim 17$ – $35 \mu\text{m}$  and  $E$  detectors of  $\sim 300$ – $1000 \mu\text{m}$  were used. A schematic of the detector arrangement and the measured spectra is shown in Fig. 1. The angular resolutions of the detectors were  $0.4^\circ$  and  $1.8^\circ$  for forward and backward telescopes, respectively. The dead times of different electronic channels were measured by acquiring

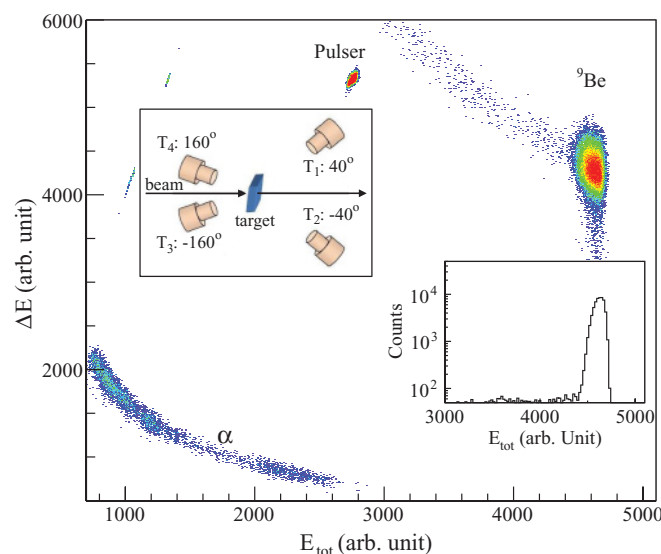


FIG. 1. (Color online) A typical two-dimensional spectrum of  $\Delta E$  vs  $E_{\text{tot}}$  for  ${}^9\text{Be} + {}^{208}\text{Pb}$  at  $E_{\text{lab}} = 34 \text{ MeV}$  and  $\theta_{\text{lab}} = 160^\circ$ . The left and right insets show the schematic of experimental setup and the projected spectrum of the  ${}^9\text{Be}$  band onto the  $x$  axis, respectively.

test pulses from a pulse generator fed to the preamplifiers of each detector and counting them directly using scalars. It was found to be in the range of 0.3–0.8 %.

To measure the deviation of elastic data from Rutherford scattering at the backward angle as a function of energy we defined the ratio  $R(E)$  [23] as

$$R(E) = \frac{\sqrt{Y_3(E)Y_4(E)}}{\sqrt{Y_1(E)Y_2(E)}} \bigg/ \frac{\sqrt{Y_3(E_0)Y_4(E_0)}}{\sqrt{Y_1(E_0)Y_2(E_0)}}, \quad (1)$$

where  $Y_1(E)$ ,  $Y_2(E)$ ,  $Y_3(E)$ , and  $Y_4(E)$  are the dead time corrected measured elastic yields from the telescopes  $T_1$ ,  $T_2$ ,  $T_3$ , and  $T_4$ , respectively, at beam energy  $E$ . The lowest beam energy in the present measurement, 24 MeV, was taken as the reference energy ( $E_0$ ), which is much below the Coulomb barrier ( $V_B \sim 40 \text{ MeV}$  [24]). The effect due to beam wandering in the horizontal plane was minimized by taking the geometrical mean of the yields of the two forward ( $T_1, T_2$ ) and two backward ( $T_3, T_4$ ) telescopes, respectively. The uncertainties due to the target thickness and beam current were eliminated by taking the ratio of the geometric means of the backward to forward yields. Solid angle uncertainties were eliminated by normalizing these ratios to that at the lowest energy. Using this procedure the systematic uncertainties were minimized and the uncertainty in  $R(E)$  arises only due to counting statistics, which is of the order of  $\pm 0.2\%$ . This procedure is similar to that followed in measuring the dipole polarizability of  ${}^7\text{Li}$  [19] and deuteron [23].

The breakup and transfer coupling effects have to be understood in detail in order to explain the elastic scattering data at energies below the Coulomb barrier. The continuum discretized coupled channel (CDCC) and coupled reaction channel (CRC) calculations were carried out using the code FRESKO [25], version FRES 2.7. Calculations have been performed considering  ${}^9\text{Be}$  as  $\alpha + {}^5\text{He}$  and  $n + {}^8\text{Be}$  clusters. In the  $\alpha + {}^5\text{He}$  cluster picture of  ${}^9\text{Be}$ , the ground state of  ${}^9\text{Be}$  ( $\frac{3}{2}^-$ ) was constructed by taking the relative angular momentum  $L = 0$  as well as  $L = 2$  between  $\alpha$  ( $0^+$ ) and  ${}^5\text{He}$  ( $\frac{3}{2}^-$ ) clusters, with the potential taken from Ref. [26]. The  $L = 2$  component was taken in order to account for the reorientation of the highly deformed  ${}^9\text{Be}$  nucleus. In addition to the ground state, the  $\frac{5}{2}^-$  inelastic state at energy 2.429 MeV and the  $\frac{7}{2}^-$  resonance state at 6.38 MeV were generated using the  $\alpha + {}^5\text{He}$  cluster model. The breakup calculations including these states along with the  $\alpha + {}^5\text{He}$  continuum were performed. The  $\alpha + {}^5\text{He}$  continuum model space in momentum was limited to  $0 \leq k \leq 0.8 \text{ fm}^{-1}$  with  $\Delta k = 0.1 \text{ fm}^{-1}$ .

In the other cluster model, an  $n + {}^8\text{Be}$  cluster picture of  ${}^9\text{Be}$  was used. The potential parameters (radius and diffuseness) along with a spin-orbit component for the binding of  $n$  in  ${}^9\text{Be}$  has been taken from Ref. [27]. A depth of 44.9 MeV for the volume potential was found to reproduce the binding energy. The  ${}^9\text{Be}/{}^8\text{Be}$  overlap spectroscopic factor  $C^2S = 0.42$  [27] was used. The nonresonant continuum and the resonance states 1.78 ( $\frac{1}{2}^+$ ) and 3.04 ( $\frac{3}{2}^+$ ) MeV have been generated in this cluster model calculation starting with the same potential parameters as the ground state. The depth of the potential was adjusted to reproduce the resonances at correct resonance energies. The generated  $B(E1)$  strengths of the resonance

states and continuum give reasonable agreement with the measured  $(\gamma, n)$  cross section [9]. The final CDCC calculation was performed by including these resonance states and the nonresonant continuum.

The interaction potentials between  ${}^9\text{Be}$  and  ${}^{208}\text{Pb}$  were obtained by folding the fragment target potentials  $\alpha + {}^{208}\text{Pb}$  and  ${}^5\text{He} + {}^{208}\text{Pb}$  in the first model and  $n + {}^{208}\text{Pb}$  and  ${}^8\text{Be} + {}^{208}\text{Pb}$  in the second model. The  $\alpha + {}^{208}\text{Pb}$  and  ${}^5\text{He} + {}^{208}\text{Pb}$  optical potentials were taken from Ref. [18].  ${}^8\text{Be} + {}^{208}\text{Pb}$  and  $n + {}^{208}\text{Pb}$  optical potentials were taken from the fits to the  ${}^9\text{Be} + {}^{208}\text{Pb}$  elastic scattering at beam energy  $E = 68$  MeV using the Wood-Saxon form for the real and imaginary potentials. Calculated elastic scattering angular distributions with bare potential at  $E = 38$  and 44 MeV are shown in Fig. 2 (dot-dashed line).

We have performed the CRC calculations for the single neutron stripping  ${}^{208}\text{Pb}({}^9\text{Be}, {}^8\text{Be})$  channel to study the effect of this channel on elastic scattering. The following states of  ${}^{209}\text{Pb}$ : ground state ( $\frac{9}{2}^+$ ), 0.78 ( $\frac{11}{2}^+$ ), 1.42 ( $\frac{15}{2}^-$ ), 1.57 ( $\frac{5}{2}^+$ ), 2.03 ( $\frac{1}{2}^+$ ), 2.49 ( $\frac{7}{2}^+$ ), and 2.54 ( $\frac{3}{2}^+$ ) MeV were included in the calculations. The spectroscopic factors for all these single particle states were taken from Ref. [28]. The same bare potential, as used in the CDCC calculations, was used.

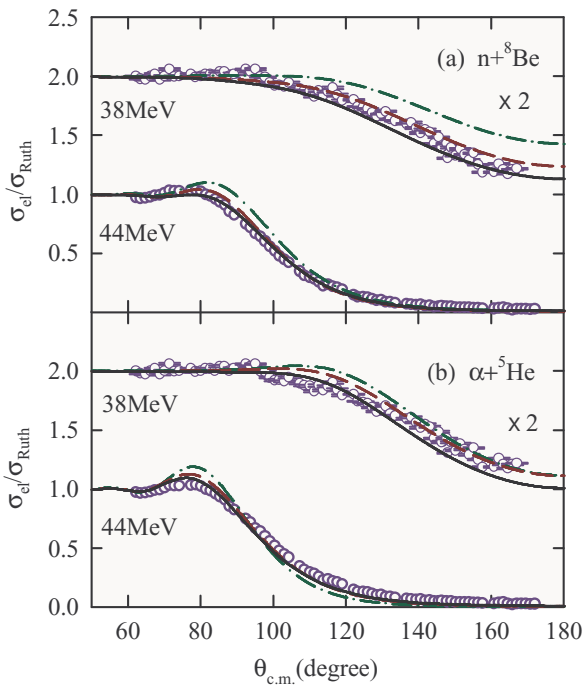


FIG. 2. (Color online) The elastic scattering angular distribution for  ${}^9\text{Be} + {}^{208}\text{Pb}$  at  $E_{\text{lab}} = 38$  and 44 MeV. The data are taken from Ref. [20]. For clarity, data, and calculations at energy  $E_{\text{beam}} = 38$  MeV have been multiplied by a factor of 2. (a) The calculations with bare potential,  ${}^9\text{Be} \rightarrow n + {}^8\text{Be}$  breakup alone, and breakup plus  ${}^{208}\text{Pb}({}^9\text{Be}, {}^8\text{Be}){}^{209}\text{Pb}$  transfer are denoted by the dot-dashed, dashed, and solid lines, respectively. (b) The calculations with bare potential,  ${}^9\text{Be} \rightarrow \alpha + {}^5\text{He}$  breakup alone, and breakup plus  ${}^{208}\text{Pb}({}^9\text{Be}, {}^8\text{Be}){}^{209}\text{Pb}$  transfer are denoted by the dot-dashed, dashed, and solid lines, respectively.

The effect of breakup and transfer couplings on the elastic scattering angular distribution are shown in Fig. 2. In Fig. 2(a) results corresponding to  $n + {}^8\text{Be}$  cluster model calculations at beam energies 38 and 44 MeV show that agreement with the data [21] is as good as that for the  $\alpha + {}^5\text{He}$  cluster model calculations shown in Fig. 2(b). While the effect of  ${}^9\text{Be} \rightarrow n + {}^8\text{Be}$  breakup coupling is to reduce the cross section [dashed line Fig. 2(a)] at all angles, in the case of  ${}^9\text{Be} \rightarrow \alpha + {}^5\text{He}$  breakup coupling, the effect is to reduce the Coulomb rainbow while increasing the cross section at backward angles [dashed line Fig. 2(b)]. However, the coupling of single neutron stripping channels reduces the elastic scattering cross section (solid line in Fig. 2) at all angles and thus improves agreement with the data.

The calculated breakup and transfer cross sections are shown in Fig. 3. The dashed curve in Fig. 3(a) denotes the  ${}^9\text{Be} \rightarrow \alpha + {}^5\text{He}$  breakup cross section, which is about one-third of the measured data at beam energies above the Coulomb barrier and one-tenth below the barrier. The solid curve in Fig. 3(a) denotes the  ${}^9\text{Be} \rightarrow n + {}^8\text{Be}$  breakup cross section, in good agreement with the data in the whole energy range, supporting the importance of the  $n + {}^8\text{Be}$  cluster structure for the breakup processes. The dashed and solid curves in Fig. 3(b) are the calculated transfer cross section using the interaction potentials derived from the  $\alpha + {}^5\text{He}$  and  $n + {}^8\text{Be}$  cluster models, respectively. Both the calculations give equally good descriptions of the measured data.

The measured ratio,  $R(E)$ , of the elastic scattering cross section at energies below the Coulomb barrier is shown in Fig. 4. Figures 4(a) and 4(b) correspond to the calculations considering the  $n + {}^8\text{Be}$  and  $\alpha + {}^5\text{He}$  cluster models, respectively. The dot-dashed line in Fig. 4 represents the calculated  $R(E)$  with the bare potential without any breakup or transfer coupling. The dashed line represents the results

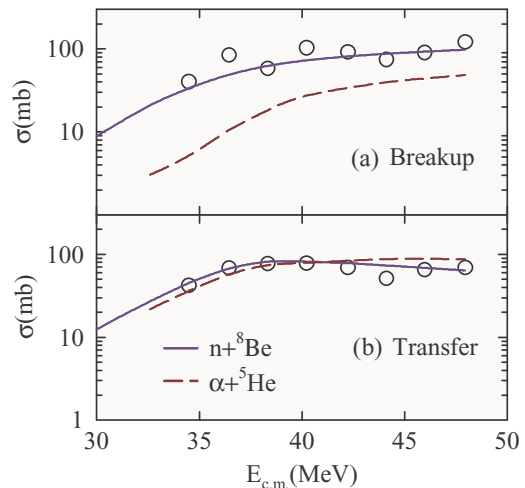


FIG. 3. (Color online) Calculated breakup and transfer cross sections. (a)  ${}^9\text{Be} \rightarrow \alpha + {}^5\text{He}$  and  ${}^9\text{Be} \rightarrow n + {}^8\text{Be}$  breakup cross sections denoted by the dashed and solid lines, respectively. (b) Calculated  ${}^{208}\text{Pb}({}^9\text{Be}, {}^8\text{Be}){}^{209}\text{Pb}$  transfer cross sections using  $\alpha + {}^5\text{He}$  and  $n + {}^8\text{Be}$  cluster models are represented by dashed and solid lines, respectively. Breakup and transfer cross section data (open circles) are taken from Ref. [21].

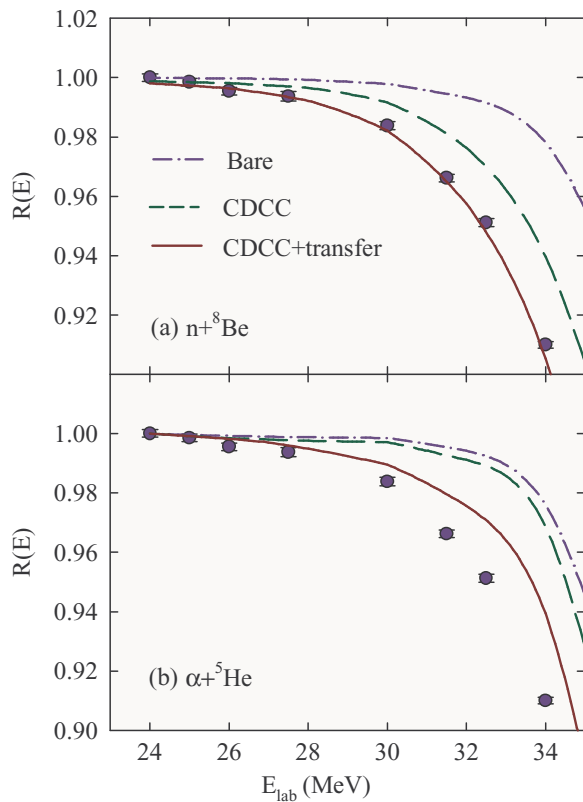


FIG. 4. (Color online) The measured ratio,  $R(E)$ , of the elastic scattering cross section (see text) at energies below the Coulomb barrier ( $V_B = 40$  MeV). The calculations with bare potential, breakup coupling only, and breakup plus  $^{208}\text{Pb}(^9\text{Be}, ^8\text{Be})^{209}\text{Pb}$  transfer are denoted by the dot-dashed, dashed, and solid lines, respectively.

obtained from the CDCC calculation considering the breakup couplings only. It can be seen that the effect of the  $^9\text{Be} \rightarrow \alpha + ^5\text{He}$  breakup coupling is very small ( $\sim \frac{1}{10}$ ) compared to the effect of the  $^9\text{Be} \rightarrow n + ^8\text{Be}$  breakup coupling. From the breakup measurement of  $^9\text{Be}$ , the extracted breakup yields into different channels show the significance of the  $^9\text{Be} \rightarrow \alpha + ^5\text{He}$  decay mode for states at higher excitation energy ( $E_{\text{ex}} > 4.0$  MeV) [5]. However, the coupling effect on elastic scattering cross sections for these states are found to be

insignificant. The solid line corresponds to the CDCC and CRC calculations performing simultaneously for the breakup along with the single neutron stripping  $^{208}\text{Pb}(^9\text{Be}, ^8\text{Be})$ . It is observed that the  $1/2^+$  resonance and  $s$ -wave continuum have the dominant coupling effect on the elastic scattering. Surprisingly, the transfer channel has a significant effect,  $\sim 1\%$  even at 10 MeV below the barrier. It is clear from Fig. 4 that the measured high precision ratio  $R(E)$  can only be explained by the  $n + ^8\text{Be}$  cluster model. The low breakup threshold, 1.67 MeV, for  $^9\text{Be} \rightarrow n + ^8\text{Be}$  and the strong  $E1$  coupling of the  $1/2^+$  resonance lying just 110 KeV above the threshold results in the dominance of the  $n + ^8\text{Be}$  model. By using the method described in Ref. [19], the dipole polarizability of  $^9\text{Be}$  is estimated to be  $\alpha_0 = 0.12$  and  $0.88 \text{ fm}^3$  for the  $\alpha + ^5\text{He}$  and  $n + ^8\text{Be}$  cluster structures, respectively.

In summary, we have carried out high precision elastic scattering measurement and investigated the sensitivity of the data to the underlying cluster structure of the weakly bound nucleus  $^9\text{Be}$ . The precision measurement of the elastic scattering cross section has been used to obtain the ratio  $R(E)$  with statistical uncertainty of  $\pm 0.2\%$  over a range of energies 24–34 MeV. The CDCC calculations for the  $^9\text{Be} + ^{208}\text{Pb}$  system using  $\alpha + ^5\text{He}$  and  $n + ^8\text{Be}$  cluster pictures of  $^9\text{Be}$  have been carried out. The elastic and reaction cross sections were reproduced by performing the CDCC and CRC calculations. The present work shows that the main contribution to the coupling effects on elastic scattering is due to  $1/2^+$  resonance,  $s$ -wave continuum, and single neutron stripping channels. From the measured ratio  $R(E)$  and the theoretical framework used, we are able to discriminate between the two cluster models, and the  $n + ^8\text{Be}$  cluster structure of  $^9\text{Be}$  is found to be more appropriate for describing the elastic and reaction cross sections. It will be interesting to extend this method to study the cluster structure of weakly bound nuclei, e.g.,  $^{11}\text{Be}$  and  $^{11}\text{Li}$ , in which coupling effects are expected to be larger.

The authors would like to thank the operation staff of the Pelletron Accelerator for providing high quality beam during the experiment. The help during the experiment from P. Patale is gratefully acknowledged. We thank Professor N. Keeley and Professor V. M. Datar for their helpful suggestions regarding the calculations.

- [1] B. S. Meyer, G. J. Mathews, W. M. Howard, S. E. Woosley, and R. D. Hoffman, *Astrophys. J.* **399**, 656 (1992).
- [2] M. Hirai, S. Kumano, K. Saito, and T. Watanabe, *Phys. Rev. C* **83**, 035202 (2011).
- [3] J. Seely *et al.*, *Phys. Rev. Lett.* **103**, 202301 (2009).
- [4] M. Freer, *Rep. Prog. Phys.* **70**, 2149 (2007).
- [5] T. A. D. Brown, P. Papka, B. R. Fulton, D. L. Watson, S. P. Fox, D. Groombridge, M. Freer, N. M. Clarke, N. I. Ashwood, N. Curtis, V. Ziman, P. McEwan, S. Ahmed, W. N. Catford, D. Mahboub, C. N. Timis, T. D. Baldwin, and D. C. Weisser, *Phys. Rev. C* **76**, 054605 (2007).
- [6] B. R. Fulton, R. L. Cowin, R. J. Woolliscroft, N. M. Clarke, L. Donadille, M. Freer, P. J. Leask, S. M. Singer, M. P. Nicoli, B. Benoit, F. Hanappe, A. Ninane, N. A. Orr, J. Tillier, and L. Stuttg e, *Phys. Rev. C* **70**, 047602 (2004).
- [7] P. Papka, T. A. D. Brown, B. R. Fulton, D. L. Watson, S. P. Fox, D. Groombridge, M. Freer, N. M. Clarke, N. I. Ashwood, N. Curtis, V. Ziman, P. McEwan, S. Ahmed, W. N. Catford, D. Mahboub, C. N. Timis, T. D. Baldwin, and D. C. Weisser, *Phys. Rev. C* **75**, 045803 (2007).
- [8] R. Rafiei, R. du Rietz, D. H. Luong, D. J. Hinde, M. Dasgupta, M. Evers, and A. Diaz-Torres, *Phys. Rev. C* **81**, 024601 (2010).
- [9] H. Utsunomiya, Y. Yonezawa, H. Akimune, T. Yamagata, M. Ohta, M. Fujishiro, H. Toyokawa, and H. Ohgaki, *Phys. Rev. C* **63**, 018801 (2000).
- [10] O. Burda, P. von Neumann-Cosel, A. Richter, C. Forss en, and B. A. Brown, *Phys. Rev. C* **82**, 015808 (2010).
- [11] W. Zahn, *Nucl. Phys. A* **269**, 138 (1976).
- [12] K. Arai, Y. Ogawa, Y. Suzuki, and K. Varga, *Phys. Rev. C* **54**, 132 (1996).

- [13] K. Arai, P. Descouvemont, D. Baye, and W. N. Catford, *Phys. Rev. C* **68**, 014310 (2003).
- [14] P. Descouvemont, *Eur. Phys. J. A* **12**, 413 (2001).
- [15] E. Garrido, D. V. Fedorov, and A. S. Jensen, *Phys. Lett. B* **684**, 132 (2010).
- [16] R. Álvarez-Rodríguez, H. O. U. Fynbo, A. S. Jensen, and E. Garrido, *Phys. Rev. Lett.* **100**, 192501 (2008).
- [17] V. Jha and S. Kailas, *Phys. Rev. C* **80**, 034607 (2009).
- [18] N. Keeley, N. Alamanos, K. Rusek, and K. W. Kemper, *Phys. Rev. C* **71**, 014611 (2005).
- [19] V. V. Parkar, V. Jha, B. J. Roy, S. Santra, K. Ramachandran, A. Shrivastava, A. Chatterjee, S. R. Jain, A. K. Jain, and S. Kailas, *Phys. Rev. C* **78**, 021601(R) (2008).
- [20] R. J. Woolliscroft, B. R. Fulton, R. L. Cowin, M. Dasgupta, D. J. Hinde, C. R. Morton, and A. C. Berriman, *Phys. Rev. C* **69**, 044612 (2004).
- [21] R. J. Woolliscroft, N. M. Clarke, B. R. Fulton, R. L. Cowin, M. Dasgupta, D. J. Hinde, C. R. Morton, and A. C. Berriman, *Phys. Rev. C* **68**, 014611 (2003).
- [22] C. Signorini, A. Yoshida, Y. Watanabe, D. Pierroutsakou, L. Stroe, T. Fukuda, M. Mazzocco, N. Fukuda, Y. Mizoi, M. Ishihara, H. Sakurai, A. Diaz-Torres, and K. Hagino, *Nucl. Phys. A* **735**, 329 (2004).
- [23] N. L. Rodning, L. D. Knutson, W. G. Lynch, and M. B. Tsang, *Phys. Rev. Lett.* **49**, 909 (1982).
- [24] A. Gómez Camacho, E. F. Aguilera, and A. M. Moro, *Nucl. Phys. A* **762**, 216 (2005).
- [25] I. J. Thompson, *Comput. Phys. Rep.* **7**, 167 (1988).
- [26] N. Keeley, K. W. Kemper, and K. Rusek, *Phys. Rev. C* **64**, 031602(R) (2001).
- [27] J. Lang, R. Müller, J. Unternährer, L. Jarczyk, B. Kamys, and A. Strzalkowski, *Phys. Rev. C* **16**, 1448 (1977).
- [28] D. G. Kovar, Nelson Stein, and C. K. Bockelman, *Nucl. Phys. A* **231**, 266 (1974).